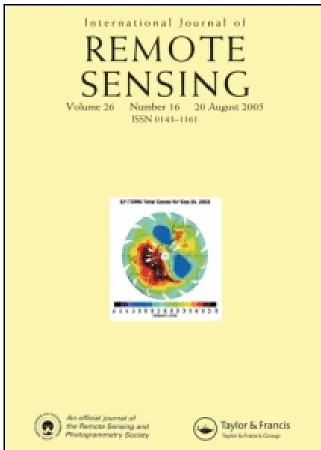

International Journal of Remote Sensing
Publication details, including instructions for authors and subscription information:
http://www.informaworld.com/smpp/title~content=t713722504

An approximate model for the microwave brightness temperature of the sea

A. Guissard [a]; P. Sobieski [a]
[a] Laboratoire de Télécomunications et d'Hyperfréquences, Université Catholique de Louvain, Bā axwell, Louvain-la-Neuve, Belgium

Online Publication Date: 01 November 1987

To cite this Article: Guissard, A. and Sobieski, P. (1987) 'An approximate model for the microwave brightness temperature of the sea', International Journal of Remote Sensing, 8:11, 1607 — 1627

To link to this article: DOI: 10.1080/01431168708954802
URL: http://dx.doi.org/10.1080/01431168708954802

INT. J. REMOTE SENSING, 1987, VOL. 8, NO. 11, 1607–1627

An approximate model for the microwave brightness temperature of the sea

A. GUISSARD and P. SOBIESKI

Laboratoire de Télécomunications et d'Hyperfréquences,
Université Catholique de Louvain, Bâtiment Maxwell,
1348 Louvain-la-Neuve, Belgium

Abstract. A modified two-scale model is proposed for scattering and emissivity calculations for certain classes of random rough surfaces. It is based on an approach by Burrows and by Brown, but it has been extended to bistatic scattering by lossy dielectric surfaces, and it incorporates modified Fresnel reflection coefficients and a simple correction for multiple-scattering effects. The method is shown to be applicable to the ocean surface for light and moderate winds. A contracted form of the radiative-transfer equation is proposed and the included Wentz correction for surface scattering is discussed. This could lead to a method that could be both simple and accurate enough for real-time inversion algorithms in microwave remote sensing.

1. Introduction

Rigorous determination of the microwave scattering and emission properties of the ocean surface remains an open problem. Reliable models would, however, be quite useful in order to improve the accuracy of the inversion methods that are needed in all remote-sensing applications, at the basic condition that they would be efficient from the point of view of numerical calculations, if real-time processing is required. Moreover it is known that higher accuracy is necessary for emissivity calculations than for backscattering calculations, and that in the first case shadowing and multiple-scattering effects must be accounted for in order to satisfy energy-conservation requirements.

Simple two-scale models for rough-surface scattering are not satisfactory when applied to the ocean surface. More rigorous methods, including multiple scattering, lead to unacceptable computer times. A method that could be both rigorous enough and computer-efficient for surfaces that are good, although not perfect, conductors is the boundary-perturbation method of Burrows (1973), as applied by Brown (1978) to backscattering by a perfect conductor. It is extended here to bistatic scattering by a lossy dielectric interface and combined with the use of modified Fresnel reflection coefficients and with a correction for multiple-scattering effects.

This method has been applied to the ocean surface, described by its slope probability density function and vertical-displacement spectrum, in order to obtain the surface emissivity. A contracted form of the radiative-transfer equation for the brightness temperature as measured by a spaceborne radiometer is proposed here; it is amenable to simple approximations. This equation is based on a suggestion by Grody (1976), as modified by Guissard (1983), and further modified here by including a scattering correction factor first proposed by Wentz (1983). It is shown that the correction factor of Wentz does not depend only on the wind friction velocity u_*, as he assumed, but on other parameters as well, and that the dependence on u_* is not linear. The present analysis is only concerned with rough open sea; foam effects have not yet been included owing to the lack of an adequate modelling.

2. Boundary-perturbation method of Burrows

Let us consider a rough surface whose mean value is the horizontal plane XOY and that separates air (above) from an arbitrary medium (below). Let us represent the surface by the equation

$$z = \zeta(x, y) \tag{1}$$

The method of Burrows (1973) is based on the assumption that the surface can be considered as the superposition of a large-scale (or 'filtered') component ζ_F and a small scale component (or 'ripples') ζ_R in such a way that

$$k\sigma_R \ll 1 \tag{2}$$

where σ_R is the r.m.s. displacement of the ripples, defined by

$$\sigma_R^2 = \langle |\zeta_R|^2 \rangle \tag{3}$$

and k is the wavenumber of the incident electromagnetic wave.

Let $\mathbf{E}^s$ be the field scattered in the direction of the unit vector $\hat{\mathbf{s}}$, when an incident field $\mathbf{E}^i$ (a plane wave) is incident from the direction $\hat{\mathbf{i}}$ (see figure 1). The directions $\hat{\mathbf{i}}$ and $\hat{\mathbf{s}}$ are defined by their spherical coordinates (θ_i, ϕ_i) and (θ_s, ϕ_s). The scattered field is evaluated as the expansion

$$\mathbf{E}^s = \mathbf{E}^{(0)} + \mathbf{E}^{(1)} + \mathbf{E}^{(2)} + \ldots \tag{4}$$

with respect to the small parameter σ_R. The first term $\mathbf{E}^{(0)}$ is the field scattered when the ripples are completely removed. The second term is of first order in σ_R, and the method will be efficient only if the expansion can be truncated after this term. Let us show that $\mathbf{E}^{(1)}$ can be found directly from an application of the reciprocity theorem.

An auxiliary current source $\mathbf{J}'$ is introduced in the form of an electric dipole $\mathbf{J}'$

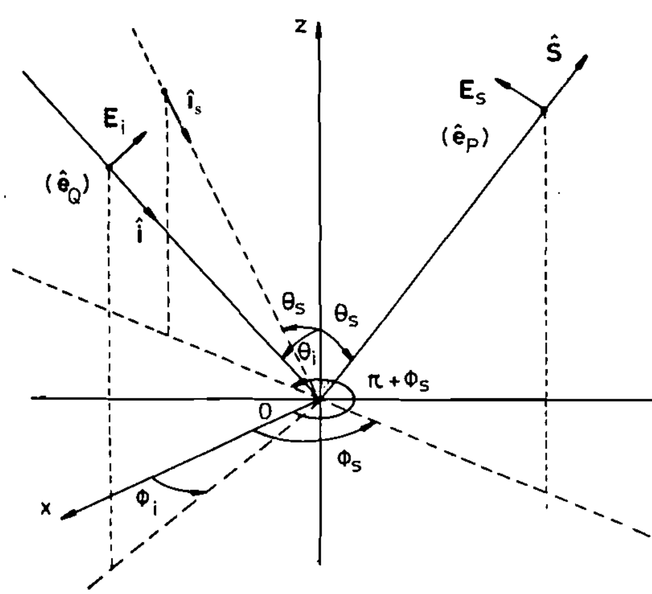

Figure 1. The basic geometry for scattering calculations.

$=\mathbf{J}'_0\delta(r-r')$; it generates fields $\mathbf{E}'$ and $\mathbf{H}'$. Let S_0 be the unperturbed boundary and S be the exact surface; let V be the (small) volume contained between S_0 and S, and let $\zeta_R^\perp$ be the ripple displacement measured along the normal to S_0. Form reciprocity, one finds that

$$\mathbf{E}^{(1)}\cdot\mathbf{J}'_0=\iint_{S_0}(\mathbf{E}'\cdot\mathbf{J}-\mathbf{H}'\cdot\mathbf{J}_m)|\zeta_R^\perp|\,dS_0 \tag{5}$$

where $\mathbf{J}$ and $\mathbf{J}_m$ are appropriate electric and magnetic sources located within V and given by

$$\mathbf{J}=j\omega(\varepsilon-\varepsilon_0)\mathbf{E}_2,\quad \mathbf{J}_m=j\omega(\mu-\mu_0)\mathbf{H}_2 \tag{6}$$

Here ε and μ are the relative permittivity and permeability of the medium below the surface, $\mathbf{E}_2$ and $\mathbf{H}_2$ are the field values just below the surface, and $j^2=-1$. Substituting these sources into (5), the result of Burrows (1973) for the first-order perturbation is obtained. For a lossy dielectric (like sea water), the second term in (5) is identically zero.

Now let the incident electric field have unit amplitude and polarization state defined by the unit vector $\hat{\mathbf{e}}_Q$. Assuming that the auxiliary source $\mathbf{J}'_0$ is at a large distance R from the scattering surface, the electric field from $\mathbf{J}'_0$ is transformed into an equivalent plane wave of unit amplitude and polarization state $\hat{\mathbf{e}}_P$. Then, from (5), the P-component of the scattered field $E_{PQ}^{(1)}$ is obtained as

$$E_{PQ}^{(1)}=k^2G(R)\iint_A\frac{1}{\varepsilon_0}(\mathbf{D}'\cdot\Delta\mathbf{E}-\mathbf{E}'\cdot\Delta\mathbf{D})\zeta_R(x,y)\,dx\,dy \tag{6}$$

where k is the electromagnetic wavenumber (in air), A is the horizontal projection of the illuminated area, ζ_R is measured along the vertical OZ axis, $G(R)=\exp(-jkr/4\pi R)$ and R is the distance from 0 to the far-field observation point in direction $\hat{\mathbf{s}}$. The fields $\mathbf{E}'$ and $\mathbf{D}'$ are the fields on the unperturbed surface S_0 due to the incident field from $-\hat{\mathbf{s}}$, while $\Delta\mathbf{E}$ and $\Delta\mathbf{D}$ are the discontinuities in the fields on the unperturbed surface S_0 due to the incident field from $\hat{\mathbf{i}}$. These fields are obtained from the zeroth-order solution (tangent-plane approximation). Since the tangential component of the electric field and the normal component of the electric displacement are continuous across the boundary, one has

$$\mathbf{D}'\cdot\Delta\mathbf{E}-\mathbf{E}'\cdot\Delta\mathbf{D}=\mathbf{D}'_n\cdot\Delta\mathbf{E}_n-\mathbf{E}'_t\cdot\Delta\mathbf{D}_t$$

where the subscripts n and t stand for the components normal and tangential to the unperturbed surface S_0. So we remember that when the fields are evaluated in the Kirchhoff approximation, they contain a phase term that is identical with the phase term of the incident plane wave. Therefore we write

$$\mathbf{E}=\mathbf{e}\exp(-jk\hat{\mathbf{i}}\cdot\mathbf{r}_0),\quad \mathbf{D}=\mathbf{d}\exp(-jk\hat{\mathbf{i}}\cdot\mathbf{r}_0)$$

$$\mathbf{E}'=\mathbf{e}'\exp(+jk\hat{\mathbf{s}}\cdot\mathbf{r}_0),\quad \mathbf{D}'=\mathbf{d}'\exp(+jk\hat{\mathbf{s}}\cdot\mathbf{r}_0)$$

where $\mathbf{r}_0$ is the vector position of a point on the surface S_0 measured from the arbitrary origin O, usually taken within the illuminated area:

$$\mathbf{r}_0=\hat{\mathbf{x}}x+\hat{\mathbf{y}}y+\hat{\mathbf{z}}\zeta_F(x,y) \tag{7}$$

and lower-case letters denote fields evaluated at the origin for unit incident fields.

Substituting these results into (6), one obtains the following expression for the first-order scattered field:

$$E_{PQ}^{(1)}=k^2G(R)\int\int_A H_{PQ}(\alpha,\beta,\varepsilon)\exp(j\mathbf{v}\cdot\mathbf{r}_0)\zeta_R(x,y)\,dx\,dy \tag{8}$$

where the vector $\mathbf{v}$ is related to the unit vectors $\hat{\mathbf{i}}$ and $\hat{\mathbf{s}}$ by

$$\mathbf{v}=\mathbf{k}(\hat{\mathbf{s}}-\hat{\mathbf{i}}) \tag{9}$$

and the function H_{PQ} is given by

$$H_{PQ}=\frac{1}{\varepsilon_0}[\mathbf{d}'_n\cdot(\mathbf{e}_{1n}-\mathbf{e}_{2n})-\mathbf{e}'_t\cdot(\mathbf{d}_{1t}-\mathbf{d}_{2t})] \tag{10}$$

with subscripts 1 and 2 standing for the fields in the media respectively above and below the surface. H_{PQ} depends on the properties of the lower medium through ε and on the slopes of the large-scale surface $\alpha=\partial\zeta_F/\partial x$ and $\beta=\partial\zeta_F/\partial y$ evaluated at $\mathbf{r}_0$; it does not depend explicitly on the position $\mathbf{r}_0$ on the surface. The expressions of the functions H_{PQ} are given in Appendix A. A result quite similar to (8) has been obtained by Brown (1981), where his functions Γ_{ab} correspond to $\frac{1}{4}$ of our H_{PQ}, with the following correspondance of the polarizations: $a\rightarrow Q$, $b\rightarrow P$. However the Γ_{ab} contain an extra factor $(\hat{\mathbf{n}}\cdot\hat{\mathbf{z}})^{-1}$, where $\hat{\mathbf{n}}$ is the local normal to the large scale surface: the difference is due to the fact that Brown uses ζ_R and not $\zeta_R^{\perp}$ in (5), which will be important when approaching grazing incidence. There also seems to be a sign error in the expression for Γ_{ab}.

3. Splitting of the surface

The above method will be useful only if the zeroth-order component of the scattered field can be easily evaluated. This would be the case if the mean radius of curvature of the large-scale surface ρ_F is large compared with the EM wavelength, i.e. if

$$k\rho_F\gg 1 \tag{11}$$

Then the field $\mathbf{E}^{(0)}$ can indeed be calculated using the Kirchhoff tangent-plane approximation combined with stationary-phase evaluation of the resulting integral (Barrick 1968 a, b). If σ_{sF} is the r.m.s. slope and l_F is the correlation length of the filtered surface then it can be shown that for a Gaussian surface (see Ulaby *et al.* 1982, Appendix 12F)

$$\rho_F\cong\frac{\sqrt{2}}{2\cdot 76}\frac{l_F}{\sigma_{sF}}\cong\frac{l_F}{2\sigma_{sF}} \tag{12}$$

provided that $\sigma_{sF}^2\ll 1$. For the sea surface, the slope of the large scale will never exceed unity (except for breaking waves), and condition (11) will necessarily be fulfilled if

$$kl_F\gg 1 \tag{13}$$

Several criteria have been suggested in the literature for separating one component of the surface from the other. Wentz (1975) selected a K_b such that $k\sigma_R$ (see (2)) be of order 0·12–0·25, and then verifies that the corresponding large-scale slope variance is small enough; no condition is set on the curvature. Following Brown (1978), we shall start from the surface-displacement spectrum with that aim in mind. Let us recall that the surface spectrum is the Fourier transform of the surface-displacement covariance

$$\gamma(K_x, K_y) = \mathrm{FT}\{\Gamma(x, y)\} \tag{14}$$

where

$$\Gamma(x, y) = \langle \zeta(x_1, y_1)\zeta(x_2, y_2) \rangle \tag{15}$$

$x = x_1 - x_2$, $y = y_1 - y_2$, and statistical homogeneity is assumed. In ocean research, the spectrum is usually normalized according to

$$\sigma^2 = \int\int_{-\infty}^{\infty} \gamma(K_x, K_y)\, dK_x\, dK_y = \Gamma(0, 0) \tag{16}$$

where σ is the surface r.m.s. displacement. A boundary value K_b of the hydrodynamic wavenumber $|\mathbf{K}| = (K_x^2 + K_y^2)^{1/2}$ is selected such that the large-scale spectrum γ_F and the small-scale spectrum γ_R are given respectively by

$$\begin{aligned} \gamma_F &= \gamma(K_x, K_y) \quad \text{for } |\mathbf{K}| \leqslant K_b \\ \gamma_R &= \gamma(K_x, K_y) \quad \text{for } |\mathbf{K}| > K_b \end{aligned} \tag{17}$$

For the large-scale surface thus defined, the correlation length l_F is of order K_b^{-1}, and the condition (13) can be replaced by

$$K_b/k \ll 1 \tag{18}$$

Two conditions thus have to be simultaneously satisfied: condition (18) and condition (2), where σ_R^2 is obtained from (16) for $\gamma = \gamma_R$. To simplify the analysis, let us introduce the constraint

$$k\sigma_R = \frac{K_b}{k} = \delta \tag{19}$$

where δ should be a small quantity. In order to investigate the applicability of the method to the ocean surface, we have chosen the spectrum proposed by Bjerkaas and Riedel (1979), which is a synthesis of many previous proposed forms and measurements. It applies to a fully developed sea and stable atmospheric conditions and depends then only on the wind friction velocity u_* as the input parameter. Curves of σ_R as a function of K_b are calculated from

$$\sigma_R^2 = \int\int \gamma(K_x, K_y)\, dK_x\, dK_y \quad \text{for } |\mathbf{K}| > K_b \tag{20}$$

and curves of σ_R for a constant electromagnetic frequency can be deduced from (19), i.e. $\sigma_R = K_b/k^2$ (*Guissard et al.* 1986). From the intersection of these curves, the values of K_b and δ are obtained. They are shown in figures 2 and 3 as functions of u_* for various frequencies. It can be seen that K_b is roughly proportional to the frequency, i.e. the filtered surface contains more and more components as the frequency increases. The ratio δ is roughly the same at all microwave frequencies considered and increases with u_*. It appears that the condition $\delta \ll 1$ will fail for very high winds ($u_* = 125\ \mathrm{cm\ s^{-1}}$ corresponds approximately to $U_{19.5} = 25\ \mathrm{m\ s^{-1}}$ under stable conditions); but for light-to-moderate winds, the method should give results of reasonable accuracy.

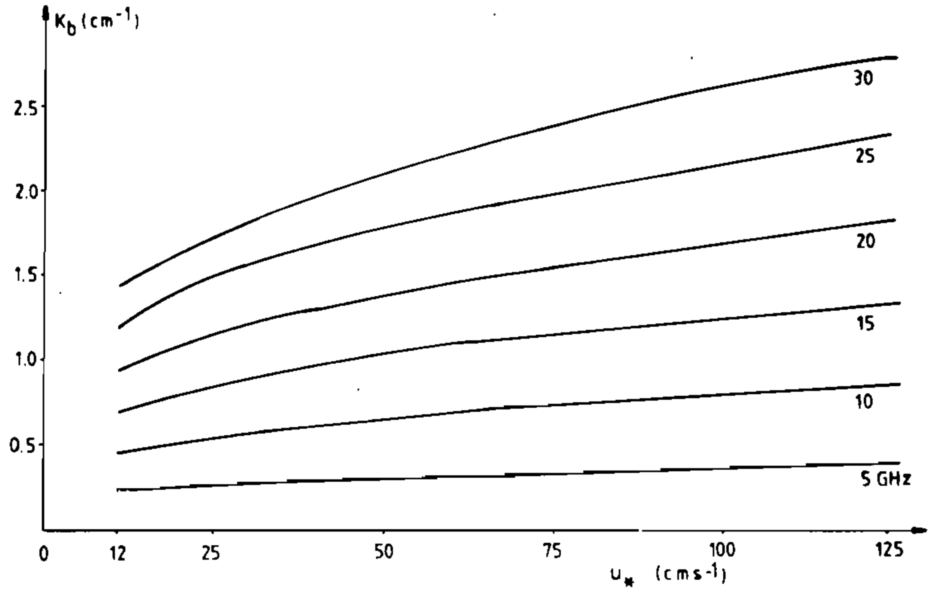

Figure 2. The boundary wavenumber K_b as a function of the wind friction velocity u_* for various electromagnetic frequencies.

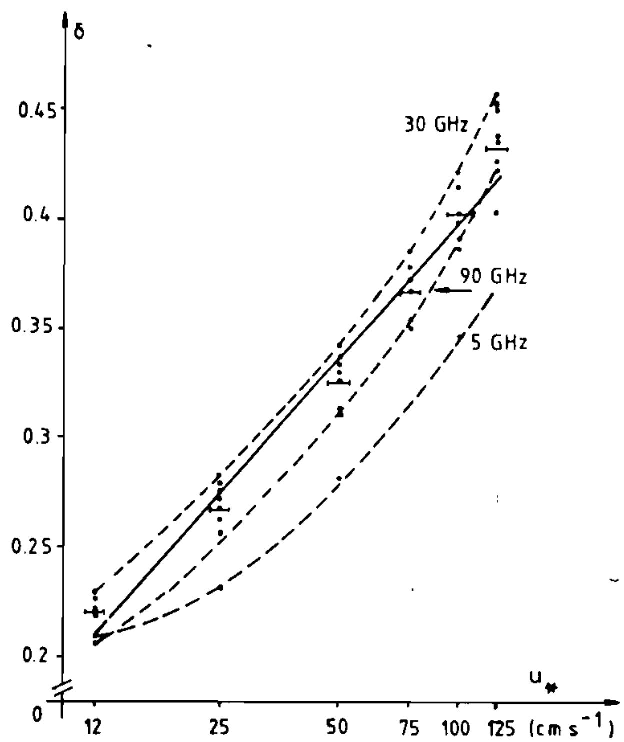

Figure 3. The quantity δ as a function of the wind friction velocity u_* is shown by dashed lines for various electromagnetic frequencies. The solid line gives the δ-values used in the calculations.

4. Bistatic scattering coefficients

The bistatic scattering coefficient (radar bistatic cross-section per unit area) is defined for a unit incident electric field with polarization $\hat{\mathbf{e}}_Q$ as (Ulaby *et al.* 1982)

$$\sigma^0_{PQ}(\hat{\mathbf{s}},\hat{\mathbf{i}})=\frac{1}{A}4\pi R^2\langle|E^s_{PQ}|^2\rangle \tag{21}$$

where A is the illuminated area and $\langle\,\rangle$ denotes an ensemble average over all realizations of the random rough surface. Using the expansion (4) limited to first order, one has

$$\langle|E^s_{PQ}|^2\rangle=\langle|E^{(0)}_{PQ}|^2\rangle+\langle|E^{(1)}_{PQ}|^2\rangle+2\mathrm{Re}\,\langle E^{(0)}_{PQ}E^{(1)*}_{PQ}\rangle \tag{22}$$

One notes that $E^{(0)}_{PQ}$ depends only on the large-scale component, while ζ_R is the only quantity in $E^{(1)}_{PQ}$ that depends on the small-scale component.

Here a final assumption is introduced, namely that ζ_F and ζ_R are statistically independent random processes. Such an assumption is not strictly correct for the ocean surface. There is indeed experimental evidence that the small capillary waves are modulated by the large gravity waves (see e.g. Shearman 1983), and the boundary wavenumber K_b (figure 2) is of the order of the critical value of $3{\cdot}6\,\mathrm{cm}^{-1}$ that separates the two types of waves. There is also experimental evidence that this modulation has an appreciable effect on radar-backscattering measurements, when the instrument resolution is high enough for the illuminated patch dimensions to be only a fraction of the surface dominant wavelength (Wright *et al.* 1980). This is the case for short-range radar measurements or for high-resolution SARs. However, in all cases where the illuminated area is large compared with the long-wave wavelength, as is the case for all radiometric measurements from the satellite-borne sensors under consideration here, it may be assumed that there is a spatial averaging process that eliminates such modulation effects. We are thus concerned with locally averaged small-scale displacements ζ_R, and the high-wavenumber part of the surface spectrum is similarly to be regarded as a locally averaged spectrum, corresponding to the assumption that the rough surface is a spatially homogeneous random process. Thus if we accept that ζ_F and this local average of ζ_R are statistically independent then we note that the last term in (22) is proportional to $\langle\zeta_R\rangle$ and will be zero since $\langle\zeta_R\rangle$ is zero by definition. As a consequence, the scattering coefficient is the sum of two contributions (to first order in σ_R):

$$\sigma^0_{PQ}=(\sigma^0_{PQ})^0+(\sigma^0_{PQ})^1 \tag{23}$$

If the correlation between ζ_F and ζ_R is not negligible, it could be accounted for by the last term in (22).

The zeroth-order term in (23) is given by the classical Kirchhoff solution for the large-scale surface, modified by the introduction of a shadowing function. It is proportional to the local reflection coefficient and to the large-scale slope probability density function (p.d.f.)$T_{sF}(\alpha,\beta)$ evaluated at the specular reflection points (Barrick 1968 a, b), where $\alpha=-v_x/v_z$, $\beta=-v_y/v_z$ (v_x, v_y, v_z are the components of the vector $\mathbf{v}$ defined in (9)). The shadowing function equals the probability that a point of the surface is both illuminated (incident shadowing function) and visible (scattering shadowing function), given the slopes at that point. A general expression of the shadowing function has been proposed by Brown (1980), under a number of assumptions, but it can be explicitly evaluated only if the surface is Gaussian, as shown by Smith (1967). The validity of the shadowing correction was recently investigated with great care for a perfectly conducting rough surface by Brown (1984). He

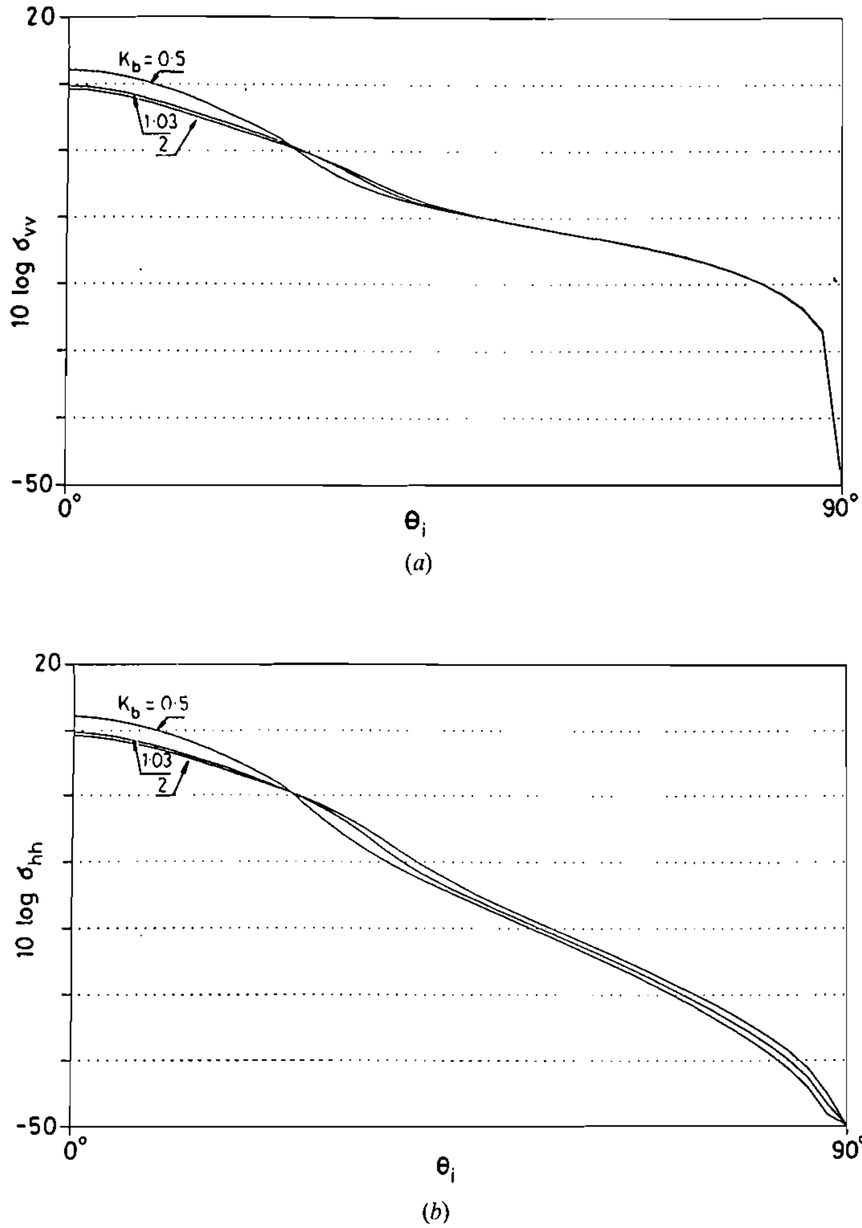

Figure 4. Backscattering coefficient as a function of angle of incidence for various values of the boundary wavenumber K_b: (a) V polarization; (b) H polarization ($u_* = 60\,\mathrm{cm\,s^{-1}}$; salinity $S = 34‰$; sea-surface temperature $= 20°\mathrm{C}$; $f = 14\,\mathrm{GHz}$; optimal $K_b = 1{\cdot}03\,\mathrm{cm^{-1}}$).

concluded that the use of the incident shadowing function can be justified but that the scattering shadowing function can lead into difficulties in those cases where the curvature of the surface is such that focusing to a shadowed point occurs. Although this might be of some concern, we do not believe that it should seriously affect emissivity calculations. Therefore, without any simple alternative approximation, we do use the concept of shadowing here in the form obtained by Smith (1967) under the acceptable assumption that the surface has Gaussian statistics.

The first-order term in (23) is evaluated by starting from Brown's solution for backscattering from a perfectly conducting surface and extending it to bistatic scattering from a lossy dielectric interface. It is observed that $(\sigma^0_{PQ})^1$ has the form of a double Fourier transform of a product of two functions, with respect to the variables x and y. This is equivalent to convolution of the transforms, and the following result is obtained, with shadowing effects included:

$$(\sigma^0_{PQ})^1 = \frac{k^4}{4\pi v_z^2} \gamma_{\mathrm{R}}(K_x, K_y) * [H_{PQ}(\alpha', \beta', \varepsilon) T_{\mathrm{sF}}(\alpha', \beta') P(\hat{\imath}; \alpha', \beta')] \tag{24}$$

where * is the convolution operation, $\alpha' = -K_x/v_z$, $\beta' = -K_y/v_z$, and $P(\hat{\imath}; \alpha, \beta)$ is the probability that a point with slopes α and β be illuminated from direction $\hat{\imath}$ and is given explicitly in Appendix B; the result of the convolution must be evaluated at $K_x = v_x$, $K_y = v_y$.

Some examples of backscattering calculations performed with the above method are shown in figure 4, for vertical (V) and horizontal (H) polarizations at 14 GHz, in order to illustrate the influence of the choice of the boundary wavenumber K_{b}. Three curves are drawn, one for the optimum wavenumber K_{b} as obtained from figure 2 and the other two for a lower and a higher K_{b} respectively. The effect of K_{b} is minimized if it is chosen near the optimum value.

Using the method developed so far, we are able to calculate the bistatic scattering coefficients for any pair of incidence direction $\hat{\imath}$ and scattering direction $\hat{\mathbf{s}}$. By an integration over the upper hemisphere over all incidence directions, we shall obtain the electromagnetic radiation, emitted and scattered, in a fixed observation direction $\hat{\mathbf{s}}$. This is explained in the next section.

5. Electromagnetic radiation

The radiation of the ocean surface is composed of two parts: a contribution emitted by the surface, depending on its emissivity and temperature, and a contribution scattered by the surface, depending on its scattering properties and on the incident radiation. Let us define the reflectivity $\Gamma_Q(\hat{\imath})$ as the scattered fraction of the incident energy in direction $\hat{\imath}$ with polarization state Q. Then, using the reciprocity property, the contribution of all incident directions $\hat{\imath}$ to direction $\hat{\mathbf{s}}$ is given by

$$\Gamma_P(-\hat{\mathbf{s}}) = \frac{1}{4\pi \cos\theta_s} \iint \sigma^0_P(\hat{\mathbf{s}}, \hat{\imath})\, d\Omega_i \tag{25}$$

where the integration is over the upper hemisphere and

$$\sigma^0_P(\hat{\mathbf{s}}, \hat{\imath}) = \sigma^0_{P\mathrm{V}}(\hat{\mathbf{s}}, \hat{\imath}) + \sigma^0_{P\mathrm{H}}(\hat{\mathbf{s}}, \hat{\imath}) \tag{26}$$

V and H corresponding to reference polarizations (generally vertical and horizontal linear polarizations). The surface emissivity in direction $\hat{\mathbf{s}}$ and polarization P is

$$e_P(\hat{\mathbf{s}}) = 1 - \Gamma_P(-\hat{\mathbf{s}}) \tag{27}$$

If $T_{\mathrm{D}}(\hat{\imath})$ represents the (unpolarized) downwelling brightness temperature at sea level from direction $\hat{\imath}$ then the scattered energy in direction $\hat{\mathbf{s}}$ and polarization P is given by the scattered brightness temperature

$$T_{\mathrm{SC}P}(\hat{\mathbf{s}}) = \frac{1}{4\pi \cos\theta_s} \iint \sigma^0_P(\hat{\mathbf{s}}, \hat{\imath})\, d\Omega_i \tag{28}$$

Accurate radiative-transfer calculations require that the principle of conservation of energy be satisfied. This in turn requires that

(i) the zeroth-order term $(\sigma_{PQ}^0)^0$ be corrected for the effect of the small ripples;
(ii) multiple-scattering effects and shadowing be properly accounted for.

Let us consider the first point. Since the surface fields are approximated by the fields on a plane tangent to the large-scale surface, they are evaluated with the Fresnel reflection coefficients for a flat plane. To account for the presence of small ripples, effective reflection coefficients can be introduced. Following the small-perturbation method first introduced by Rice (1951), Valenzuela (1970)† and Wu and Fung (1972) propose correction factors for the Fresnel coefficients. Unfortunately these factors are rather complicated functions of various parameters. Moreover, the expressions obtained by Valenzuela do not agree with those obtained by Wu and Fung.

A much simpler result can be obtained under the following assumptions:

(i) from all 'form' factors describing the surface (slopes, curvatures, higher-order derivatives), the slopes are the dominant parameters;
(ii) the surface joint displacement and slope p.d.f. at a given point are approximately normal.

It can then be shown that an effective reflection coefficient is given by (Guissard 1985)

$$R_{\rm eff} = \chi_{\rm R}(2k\cos\theta_l)R \tag{29}$$

where R is the Fresnel coefficient, θ_l is the local angle of incidence on the large-scale surface and $\chi_{\rm R}(p)$ is the characteristic function of the ripple displacements. If the small-scale surface is normal it has the form $\chi_{\rm R}(p)=\exp(-\frac{1}{2}\sigma_{\rm R}^2p^2)$, where $\sigma_{\rm R}$ is the r.m.s. ripple displacement. To apply this result in the two-scale model, we should multiply $(\sigma_{PQ}^0)^0$ by a correction factor equal to $|\chi_{\rm R}(p)|^2$, i.e.

$$C_{\rm R}(\hat{\mathbf{i}}) = \exp(-4k^2\sigma_{\rm R}^2\cos^2\theta_l) \tag{30}$$

which was previously obtained for the case of a Kirchhoff perfectly conducting surface (Beckmann and Spizzichino 1963). This factor depending on the incident direction $\hat{\mathbf{i}}$ must be introduced within the integral in (25) for reflectivity calculations.

Let us next consider the multiple-scattering contribution. In the particular case of a Kirchhoff surface, the scattering coefficient σ^0 is proportional to the slope p.d.f. The integral of this p.d.f. over all slopes is by definition unity. For a perfectly conducting surface, Γ_P in (25) should be unity. This, however, will not be the case, in general, for two reasons: the presence in the integrand of (25) of an extra geometrical factor that reduces to unity only in the particular case of normal incidence; and the fact that the domain of integration in (25) does not necessarily cover the complete domain of slopes. Thus, even in that particularly simple case, energy is not conserved, clearly because multiple-scattering effects are not accounted for.

Attempts have been made by several authors to include multiple-scattering contributions. Wentz (1975) developed a method for a two-scale model: a large set of N incident rays is considered, and for each of them the behaviour of the reflected ray is analysed for one sample among all possible realizations of the random surface. According to the author, a sampling error of less than 0·5 K for the brightness temperature requires N to be as large as 10^4. The method proposed by Fung and Eom

† See also Valenzuela (1978, equations (3·6) and (3·7)) for a correction to this paper.

Table 1. Reflectivity $(\Gamma_P)_\infty$ for a large-scale perfectly conducting rough surface from Kirchhoff tangent-plane method, with shadowing effect included at 15 GHz; upwind case.

θ_s	$u_*(\mathrm{cm\,s^{-1}})$		
	15	50	125
0°	1·000	1·000	0·9980
30°	0·9998	0·9998	0·9856
40°	0·9956	0·9968	0·9594
50°	0·9666	0·9791	0·9214

(1981) is based on the Stokes parameters and on Fourier-series expansions in the azimuth angle; it is limited to the case of a Kirchhoff surface.

We tried to set up a method that, although approximate, would lead to much shorter computations. Considering that multiple scattering is principally a geometrical effect, the zeroth-order term is corrected for multiple scattering by assuming that the sea is sufficiently close to a perfect conductor for this effect to be similar to that evaluated for the perfectly conducting case. Thus the method consists in evaluating first the reflectivity $(\Gamma_P)_\infty$ for the perfectly conducting surface and to deduce from this a correction factor for multiple scattering

$$C_M = \frac{1}{(\Gamma_P)_\infty} \tag{31}$$

which is applied to the real-sea situation.

Table 1 shows some examples of $(\Gamma_P)_\infty$ values at the frequency $f = 15$ GHz. The departure from unity becomes appreciable only at high angles of incidence and high wind speeds. By multiplying it by C_M, the reflectivity Γ_p will be exactly corrected for multiple scattering when the surface is perfectly conducting. It will be approximately corrected for the sea surface.

As an illustration, the emissivity, as obtained by the above method, including the ripple correction $C_R(\hat{\mathbf{i}})$ and the multiple-scattering correction C_M, has been drawn in figure 5 for a given wind friction velocity $u_* = 60\,\mathrm{cm\,s^{-1}}$, as a function of observation angle θ_s from the vertical for two frequencies, 20·6 and 31·4 GHz, and two linear polarizations, vertical (V) and horizontal (H). These curves present the usual trends. The emissivity at 31·4 GHz is somewhat higher than at 20·6 GHz. Emissivity in vertical polarization is an increasing function of θ_s, while in horizontal polarization it is a decreasing function of θ_s.

It is not easy to make comparisons with measurements, because data for a rough sea, without foam, for known sea conditions and corrected for atmospheric effects, are scarse in the literature. We found that the brightness-temperature measurements performed by Hollinger (1971) satisfied these conditions. Hollinger gives brightness temperatures as measured from a tower located in 60 m deep water for three frequencies and various wind conditions, and corrected for the downwelling atmospheric contribution specularly reflected from the sea. At the time of writing this paper, we had no results of calculations available at exactly the same measuring conditions as those of Hollinger. Nevertheless, in order to provide some comparison, we selected one experimental case that is close enough to one of our own calculations. This is shown in

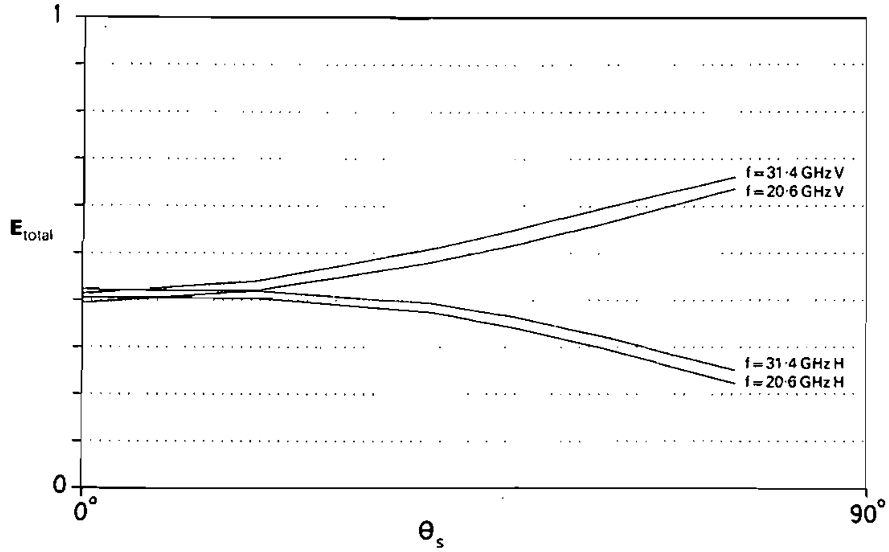

Figure 5. Emissivity of rough sea as a function of observation angle for two frequencies (20·6 and 31·4 GHz), wind friction velocity $u_* = 60\,\mathrm{cm\,s^{-1}}$, vertical (V) and horizontal (H) polarizations.

figure 6, which displays the brightness temperature emitted by the sea surface as a function of the angle of incidence for V and H polarizations. The measurements of Hollinger were made at 19·34 GHz, for wind speeds of 0·5 and 13·5 m s^{-1} at a height of 43 m, with significant wave height from 1·2 to 2·3 m. Our calculations are done at 20·6 GHz for the flat sea (specular case) and for a wind friction velocity $u_* = 60\,\mathrm{cm\,s^{-1}}$, which is equivalent to a wind speed $U_{43} = 15{\cdot}7\,\mathrm{m\,s^{-1}}$ at 43 m height, assuming a neutral atmosphere and using the Cardone (1969) model.

The agreement is not bad for *H* polarization, but the brightness temperature seems to be underestimated by our model in V polarisation. However, one should take account of the differences in frequency and in wind-speed values; there is also a difference in wave height: for a wind speed of 13·5 m at 43 m height, or a wind friction velocity of 49 cm s^{-1}, one obtains from the Bjerkaas and Riedel spectrum an r.m.s. displacement of 70 cm, i.e. a significant wave height of some 2·80 m, a value that is higher than the wave heights reported by Hollinger. Moreover, for the suppression of the atmospheric scattered contribution, the correction δ_P, to be discussed in §6 and 7, was neglected by Hollinger. Also, we do not know if neutral atmospheric stability was achieved or if the sea was fully developed (as assumed for the calculations), and swell might have been present and have modified the surface characteristics still further. Finally, the reported absolute error in brightness-temperature measurements is 5–10 per cent. In view of all these uncertainties, we may consider that the agreement between the model and the measurements is satisfactory, although more comparisons are required and some further improvement of the model is perhaps desirable.

6. Approximate radiative-transfer equation

Microwave radiometers observing the ocean from above the top of the atmosphere at various frequencies and polarizations provide a set of brightness temperatures,

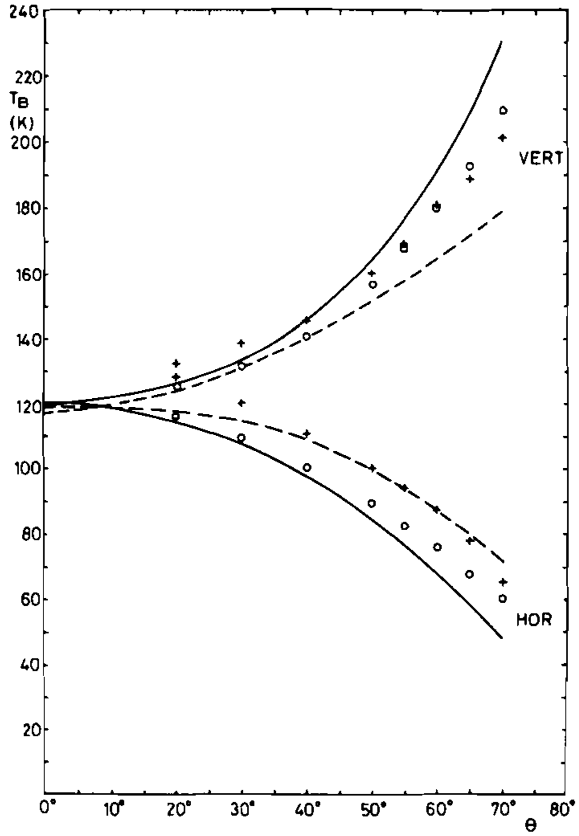

Figure 6. Comparison of brightness temperatures as deduced from Hollinger's measurements and from our model for vertical and horizontal polarizations as a function of the angle of incidence. The dots and crosses are Hollinger's results for $U_{43}=0{\cdot}5$ and $13{\cdot}5\,\mathrm{m\,s^{-1}}$ at 19·34 GHz. The solid line is the specular emissivity (flat sea), and the dashed line corresponds to our model for $u_* = 60\,\mathrm{cm\,s^{-1}}$ ($U_{43} = 15{\cdot}7\,\mathrm{m\,s^{-1}}$), both at 20·6 GHz.

which depend on both the ocean and the intervening atmosphere electromagnetic properties. The practical interest of such measurements is now well established and lies in the possibility of retrieving physical parameters, such as the wind speed, the wave height, and the water-vapour and liquid-water content, from these measurements. This implies the availability of efficient and accurate inversion procedures: one way to achieve this would be by simplifying the radiative-transfer equation (RTE). The microwave radiation from the rough boundary of a lossy dielectric and from a continuous lossy medium have been the subject of much research, particularly in the field of remote-sensing applications (Thrane 1978) and classical discussions can be found in several textbooks (e.g. Ulaby *et al.* 1982, Schanda 1986). Our aim, however, is to obtain a radiative-transfer equation written in a form that is particularly suitable for inversion purposes.

The received brightness temperature in polarization P and directions $\hat{\mathbf{s}}$ (as before, $\hat{\mathbf{s}}$ denotes the unit vector pointing from the observation point to the satellite) is given by

$$T_{BP}(\hat{\mathbf{s}}) = T_U(\hat{\mathbf{s}}) + \mathcal{T}(\hat{\mathbf{s}})[e_P(\hat{\mathbf{s}})T_s + T_{SCP}(\hat{\mathbf{s}})] \tag{32}$$

where $T_U(\hat{\mathbf{s}})$ is the contribution of the atmosphere along the upwelling path, $\mathscr{T}(\hat{\mathbf{s}})$ is the one-way atmospheric transmittance function (ratio of output power to input power) along the direction $\hat{\mathbf{s}}$, T_s is the sea-surface temperature, $e_P(\hat{\mathbf{s}})$ is the emissivity related to σ^0_{PQ} through (25) and (27), and $T_{SCP}(\hat{\mathbf{s}})$ is the scattered brightness temperature given by (28).

Let us define $\hat{\mathbf{i}}_s$ as the particular incident direction that gives specular reflection into direction $\hat{\mathbf{s}}$ (figure 1). From (25) and (28), one observes that if $T_D(\hat{\mathbf{i}})$ could be approximated by $T_D(\hat{\mathbf{i}}_s)$, the following simple result would hold:

$$T_{SCP}(\hat{\mathbf{s}}) \cong \Gamma_P(-\hat{\mathbf{s}}) T_D(\hat{\mathbf{i}}_s) = T'_{SCP}(\hat{\mathbf{s}}) \tag{33}$$

This approximation has been widely used in microwave remote sensing. In particular, Grody (1976) used it to simplify the RTE, with the further assumption that the sea-surface temperature and the atmospheric temperature at ground level T_a are equal. A similar simplified RTE was proposed by Guissard (1983), with the last assumption relaxed. It takes the form (with the $\hat{\mathbf{s}}$ dependence dropped)

$$T_{BP} = m_P T_s - \Gamma_P (T_a - T_c) \mathscr{T}^2 \tag{34}$$

where T_c is the cosmic background temperature and m_p is given by the equation

$$m_P - 1 = (1 - e_P \mathscr{T}) \frac{T_a - T_s}{T_s} - \frac{I_P}{T_s}. \tag{35}$$

In this last expression, I_P (in K) depends on the atmospheric opacity and on the vertical temperature profile. It is exactly zero for a temperature lapse rate equal to zero; for a non-zero temperature lapse rate a, it depends on the product aH, where H is the characteristic height of an assumed exponential attenuation profile, with total attenuation A. For usual temperature lapse rates and atmospheric opacities, I_P amounts to only a few K, as is shown in figure 7, where I_P is displayed as a function of the total atmospheric attenuation A (in dB) for two values of the product aH. Since T_a and T_s never differ by more than a few K, one can conclude that m_P will have values very close to unity. Written in the form (34), the RTE is a very practical expression for inversion algorithms and has been used for that purpose by the present authors, with the further inclusion of the scattering correction to be discussed below (Guissard *et al.* 1986). Detailed expressions for m_P and I_P can be found in this latter reference.

Recently, Wentz (1983) proposed to relax the assumption (33) by the introduction of a scattering correction in the RTE. The idea of Wentz is to assume that the error resulting from the approximation (33) is proportional to the approximate value T'_{SCP}

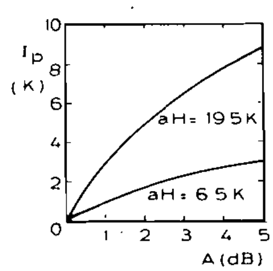

Figure 7. The correction I_P (in K) is displayed as a function of the total atmospheric attenuation A (in B) for two values of aH (a is the temperature lapse rate and H is the attenuation characteristic height).

and to write

$$T_{SCP}(\hat{\mathbf{s}}) - T'_{SCP}(\hat{\mathbf{s}}) = \Gamma_P(-\hat{\mathbf{s}}) T_D(\hat{\mathbf{i}}_s) \delta_P(\hat{\mathbf{s}}) \tag{36}$$

where $\delta_P(\hat{\mathbf{s}})$ is a dimensionless quantity, which must be small compared with unity for (33) to be a good approximation. Let us call δ_P the 'scattering correction'; it is zero for specular reflection from a perfectly flat surface. Wentz further assumes that $\delta_P(\hat{\mathbf{s}})$ is proportional to the wind friction velocity:

$$\delta_P(\hat{\mathbf{s}}) = c(f, P, \hat{\mathbf{s}}) u_* \tag{37}$$

with a proportionality factor c depending only on frequency, polarization and incidence direction (c is denoted by ω in Wentz 1983). He gives the values of c for the five SMMR frequencies: 6·6, 10·7, 18, 21 and 37 GHz (SMMR is the Scanning Multichannel Microwave Radiometer, which has been flown on board the SEASAT and Nimbus-7 spacecraft), both polarizations at an angle of incidence $\theta_s = 49°$ (from the vertical). By including the scattering correction, the scattered brightness temperature is

$$T_{SCP}(\hat{\mathbf{s}}) = \Gamma_P(-\hat{\mathbf{s}}) T_D(\hat{\mathbf{i}}_s)(1 + \delta_P(\hat{\mathbf{s}})) \tag{38}$$

and the RTE can still be written in the contracted form (34), under the condition that the correction factor m_P be slightly modified (Guissard *et al.* 1986). Note that the resulting RTE (34) does not imply any approximations and will give the exact brightness temperature if all terms on the right-hand side can be exactly calculated. In the next section the scattering correction is evaluated using the modified boundary-perturbation approach presented in the first part of this paper, and is compared with Wentz's results.

7. Parametric analysis of the scattering correction

It was logical to assume, as Wentz did, that the deviation from specular reflection increases with the surface roughness and therefore with u_*, which is a measure of the roughness. However, the correction should also depend on the atmospheric transmittance and perhaps on other parameters, for instance the sea-surface and atmospheric temperatures. Therefore a parametric analysis of δ_P has been performed in order to investigate these potential effects. The factor δ_P is obtained as the ratio

$$\delta_P(\hat{\mathbf{s}}) = \frac{\int \sigma_P^0(\hat{\mathbf{s}}, \hat{\mathbf{i}})[T_D(\hat{\mathbf{i}}) - T_D(\hat{\mathbf{i}}_s)]\, d\Omega_i}{T_D(\hat{\mathbf{i}}_s) \int \sigma_P^0(\hat{\mathbf{s}}, \hat{\mathbf{i}})\, d\Omega_i} \tag{39}$$

and depends on the sea state through $\sigma_P^0(\hat{\mathbf{s}}, \hat{\mathbf{i}})$ and on the atmosphere through $T_D(\hat{\mathbf{i}})$. Using the boundary-perturbation approach described above, including the modified Fresnel reflection coefficients and the correction factor to account for multiple scattering, δ_P has been computed for a set of sea and atmospheric conditions, and for various frequencies, incidence angle and both linear vertical (V) and horizontal (H) polarizations. In each case, two bidimensional integrations over the upper hemisphere are required to obtain the ratio δ_P. Moreover, in the numerator, the downwelling brightness temperature $T_D(\hat{\mathbf{i}})$ must be computed for each incident direction by an integration along the downwelling path.

Some results are presented in figures 8 and 9. They correspond to the frequency pair 20·6 and 31·4 GHz, which is commonly used for the retrieval of atmospheric water-vapour and cloud liquid-water contents, and to an angle of incidence of 50° (from the

Table 2. The five selected atmospheres. The opacities indicated are for a vertical path and an atmospheric temperature at ground level of 20°C.

Atm.	WV ($kg\,m^{-2}$)	LW ($kg\,m^{-2}$)	τ (dB) 20·6 GHz	31·4 GHz
1	20	0·16	0·43	0·35
2	25	0·24	0·54	0·45
3	25	0·32	0·56	0·50
4	40	0·40	0·85	0·73
5	55	0·48	1·15	0·98

vertical). The calculations have been performed for the five atmospheres defined in table 2, where WV is the integrated water-vapour content (in $Kg\,m^{-2}$), LW is the integrated cloud liquid-water content ($kg\,m^{-2}$), and the opacity τ for a vertical path is related to the transmittance $\mathscr{T}(\theta)$ along an inclined path at an angle θ from the vertical by

$$\mathscr{T}(\theta) = \exp(-\tau/\cos\theta) \tag{40}$$

The law (40) is valid for θ lower than about 80°; for higher angles of incidence, $\cos\theta$ is replaced by an exact factor accounting for the Earth's curvature. Atmospheric attenuation calculations go along the classical expressions for atmospheric gases (oxygen and water vapour) and for cloud liquid water (details can be found in Sobieski *et al.* 1986). No rain effect is considered here.

Figures 8 (*a*) and (*b*) show the dependence of the scattering correction δ_P (50°) on u_* at 20·6 and 31·4 GHz, with the opacity as a parameter. The linear Wentz correction is superimposed (Wentz's corrections at 20·6 and 31.4 GHz have been approximated for this purpose by linear interpolation from Wentz's values at 18, 21 and 37 GHz). Various conclusions may be drawn from these figures: first, the dependence of δ_P on u_* is far from being linear; secondly, the dependence of δ_P on atmospheric opacity is as important as its dependence on u_*, principally at high friction velocities. Moreover, the correction is larger and the influence of the opacity is greater for horizontal polarization than for vertical polarization. It decreases with increasing opacity: this dependence should have been expected, and implies that the approximation (33) will improve when the atmospheric contribution to the brightness temperature increases. Nevertheless, it appears that neglecting δ_P, as is commonly done when using the approximation (33), results in an error of order 10–20 per cent on the scattered contribution to the upwelling brightness temperature.

The influence of other parameters has also been investigated. Figure 9 shows the influence of the atmospheric temperature T_a at ground level for fixed values of WV and LW. The influence of T_a on δ_P is clearly related to the influence of T_a on the opacity. It appears that the sea-surface temperature has a negligible influence on δ_P.

Thus the scattering correction appears as a very useful concept to improve the purely specular approximation. However, Wentz's expression for δ_P should be improved by accounting for the non-linear dependence on u_* and for the important dependence on the atmospheric opacity. Proper modelling of δ_P will lead to more accurate retrievals of physical surface and atmospheric parameters, by inversion of the measurements obtained from spaceborne radiometers.

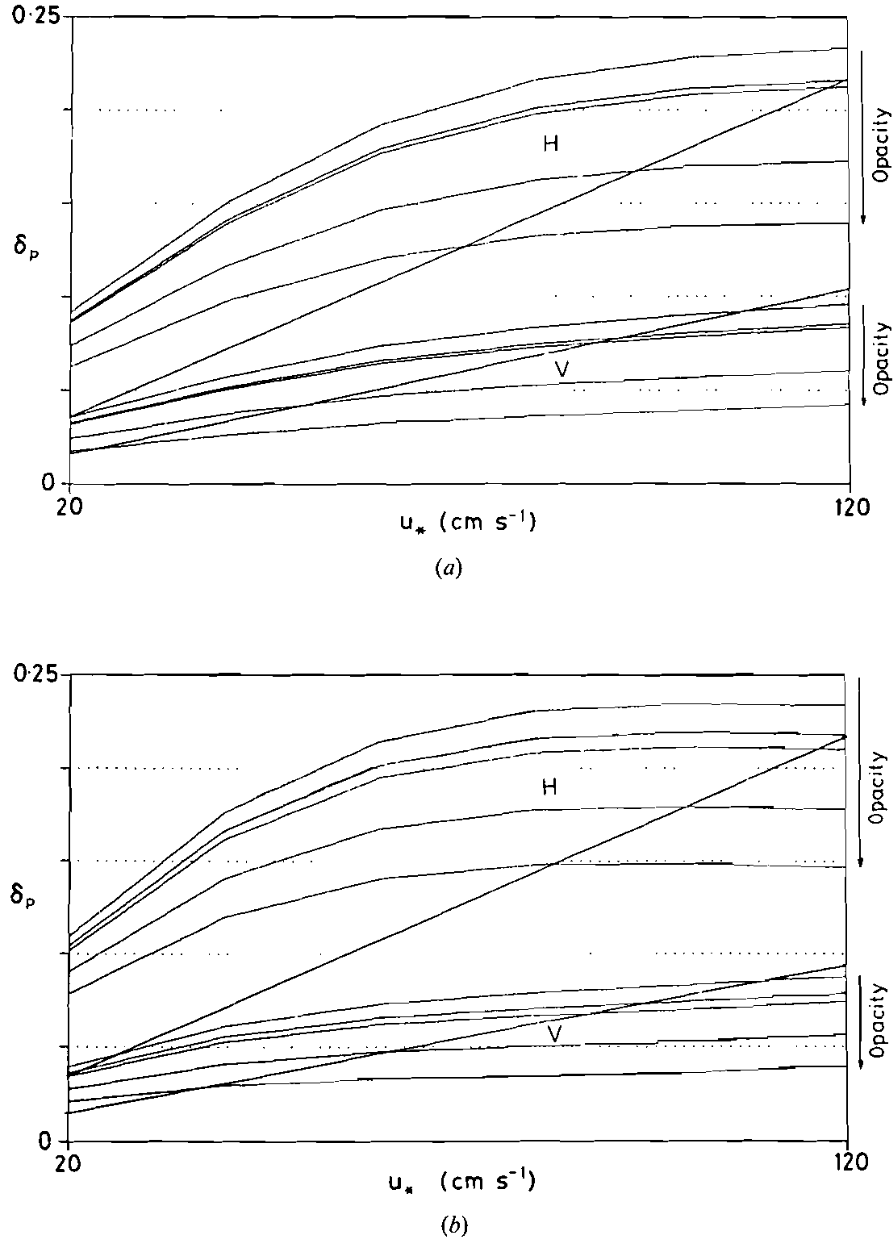

Figure 8. Scattering correction δ_p as a function of wind friction velocity u_* at an angle of incidence of 50° for the five atmospheres of table 2 and both linear polarizations: vertical (V) and horizontal (H). Increasing opacity is indicated by the direction of the arrow. The straight lines correspond to Wentz's correction. (*a*) 20·6 GHz; (*b*) 31·4 GHz.

8. Conclusion

Rigorous calculation of the microwave scattering and emission properties of the ocean surface is a difficult task. A model has been developed for calculating bistatic scattering coefficients and emissivity values of the rough surface. It is based on the

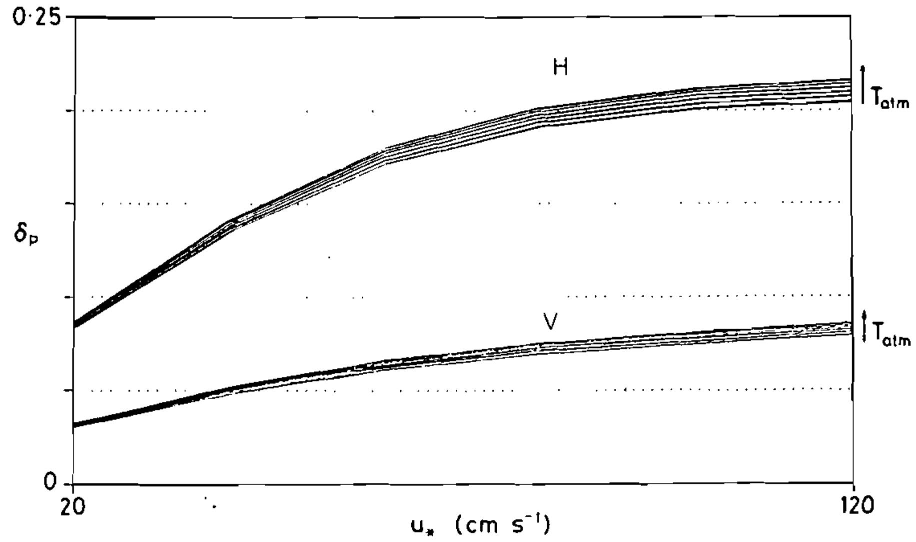

(*a*)

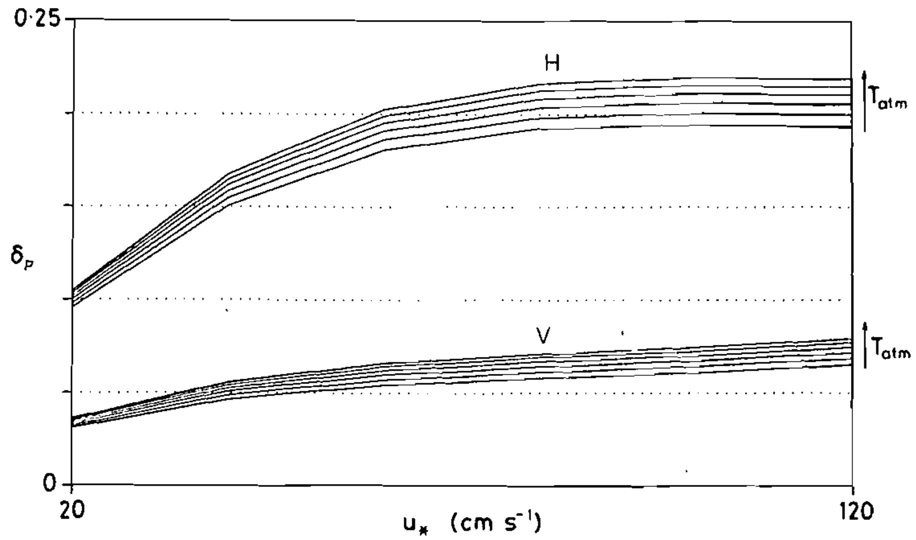

(*b*)

Figure 9. Scattering correction δ_p as a function of u_* at an angle of incidence of 50° for atmosphere no. 3, and six values of the atmospheric temperature at ground level from 5 to 30°C. Increasing temperature is indicated by the direction of the arrow. Vertical (V) and horizontal (H) polarizations. (*a*) 20·6 GHz; (*b*) 31.4 GHz.

Burrows-Brown boundary-perturbation method, in which $\sigma°$ is obtained as the sum of zeroth-order (Kirchhoff-scattering) and first-order (Bragg-scattering) terms. The method has been extended to a lossy dielectric surface and modified to approximately satisfy the conservation-of-energy criterion in emissivity calculations and to account for multiple-scattering effects in an approximate but simple way. Comparison with experimental data for the sea-surface emitted brightness temperature shows only partial agreement. The discrepancies may result from measurement errors and from a number of experimental uncertainties, as well as from residual inaccuracies in the model. Further comparisons are needed before a more definitive conclusion can be made about the accuracy of the proposed model.

The radiative-transfer equation for the upwelling brightness temperature has been presented in a contracted form that is particularly convenient for inversion purposes. It includes an atmospheric correction, accounting for the temperature lapse rate and for the vertical attenuation profile, and a surface-scattering correction. It has been shown that this surface-scattering correction does not follow the simple model proposed earlier by Wentz: it has a highly non-linear dependence on the wind friction velocity, it also depends on the atmospheric opacity, and both effects are of the same order of magnitude. Proper modelling of the scattering correction should allow improvements of the inversion algorithms from radiometric data.

Acknowledgments

Part of this work was performed under Contract 5285/82 for the European Space Agency. The authors would like to express their thanks to Christine Baufays, who performed the calculations for figures 2 and 3, and to Danielle Vanhoenacker, who participated in the development of the computer programme for scattering and emissivity calculations. Fruitful discussions with Gary S. Brown and Gaspar R. Valenzuela and the valuable comments of two anonymous reviewers are also acknowledged. Finally, many thanks are due to Edith Colle, who carefully typed and processed this paper.

Appendices A. The functions H_{PQ}

The functions H_{PQ} are evaluated on the tangent plane at an arbitrary point of the large-scale (or unperturbed) surface S_0. Let $\hat{\mathbf{n}}$ be the local normal to S_0 and let us define local v and h unit polarization vectors as follows:

$$\hat{\mathbf{e}}_{lh}=\frac{\hat{\mathbf{i}}\times\hat{\mathbf{n}}}{|\hat{\mathbf{i}}\times\hat{\mathbf{n}}|},\qquad \hat{\mathbf{e}}'_{lh}=\frac{\hat{\mathbf{s}}\times\hat{\mathbf{n}}}{|\hat{\mathbf{s}}\times\hat{\mathbf{n}}|}$$

$$\hat{\mathbf{e}}_{lv}=\hat{\mathbf{e}}_{lh}\times\hat{\mathbf{i}},\qquad \hat{\mathbf{e}}'_{lv}=\hat{\mathbf{e}}'_{lh}\times\hat{\mathbf{s}}$$

where $\hat{\mathbf{i}}$ and $\hat{\mathbf{s}}$ are the unit vectors defining the directions of incidence and scattering, as in figure 1. Let θ_l and θ'_l be the local angles of incidence for the incident and scattered directions, and let T_{vl}, T_{hl}, T'_{vl}, T'_{hl} be the local Fresnel transmission coefficients in both polarizations and for both incident and scattered waves. Then the expressions for the functions H_{PQ} are

$$H_{PQ}=(\varepsilon_r-1)\left\{(\hat{\mathbf{e}}_Q\cdot\hat{\mathbf{e}}_{lv})(\hat{\mathbf{e}}_P\cdot\hat{\mathbf{e}}'_{lv})\left(\frac{T_{vl}T'_{vl}}{\varepsilon_r^2}\right)A+(\hat{\mathbf{e}}_Q\cdot\hat{\mathbf{e}}_{lh})(\hat{\mathbf{e}}_P\cdot\hat{\mathbf{e}}'_{lh})T_{hl}T'_{hl}B+CD\right\}$$

with

$$\mathrm{A}=\varepsilon_r\sin\theta_l\sin\theta'_l+(\varepsilon_r-\sin^2\theta_l)^{1/2}(\varepsilon_r-\sin^2\theta'_l)^{1/2}B$$

$$\mathrm{B}=\hat{\mathbf{e}}_{lh}\cdot\hat{\mathbf{e}}'_{lh}$$

$$\mathrm{C}=(\hat{\mathbf{e}}_Q\cdot\hat{\mathbf{e}}_{lv})(\hat{\mathbf{e}}_P\cdot\hat{\mathbf{e}}'_{lh})T'_{hl}\left(\frac{T_{vl}}{\varepsilon_r}\right)(\varepsilon_r-\sin^2\theta_l)^{1/2}$$

$$-(\hat{\mathbf{e}}_P\cdot\hat{\mathbf{e}}'_{lv})(\hat{\mathbf{e}}_Q\cdot\hat{\mathbf{e}}_{lh})T_{hl}\left(\frac{T'_{vl}}{\varepsilon_r}\right)(\varepsilon_r-\sin^2\theta'_l)^{1/2}$$

$$\mathrm{D}=\hat{\mathbf{e}}'_{lh}\cdot(\hat{\mathbf{n}}_l\times\hat{\mathbf{e}}_{lh})$$

and where $\hat{\mathbf{e}}_Q$ and $\hat{\mathbf{e}}_P$ are the unit vectors defining the polarizations of the incident and scattered fields respectively, in the reference frame of figure 1.

B. The function $P(\hat{\mathbf{i}}; \alpha, \beta)$

The function $P(\hat{\mathbf{i}}; \alpha, \beta)$ is given by

$$P(\hat{\mathbf{i}}; \alpha, \beta) = \frac{h(\cos\theta_i - \alpha\cos\phi_i - \beta\sin\phi_i)}{1 + \Lambda(\theta_i, \phi_i)}$$

where $h(u)$ is the unit step function and θ_i, ϕ_i are the angular spherical coordinates of the incidence direction (figure 1). If the surface is Gaussian, in the sense that the height p.d.f. is jointly normal and the joint slope p.d.f. is jointly normal, the expression for $\Lambda(\theta, \phi)$ is

$$\Lambda(\theta, \phi) = \frac{1}{(2\pi)^{1/2}} \frac{w(\phi)}{\cot\theta} \exp\left(\frac{-\cot^2\theta}{2w^2(\phi)}\right) - \frac{1}{2}\operatorname{erfc}\left(\frac{\cot\theta}{\sqrt{2}\, w(\phi)}\right)$$

where

$$w^2(\phi) = \sigma_{xF}^2 \cos^2\phi + \sigma_{yF}^2 \sin^2\phi$$

σ_{xF}^2, σ_{yF}^2 are the mean-square slopes of the large scale surface along the X and Y directions respectively, and erfc is the complementary error function (Smith 1967).

References

BARRICK, D. E., 1968 a, Rough surface scattering based on the specular point theory. *IEEE Transactions on Antennas and Propagation*, **16**, 449–454.

BARRICK, D. E., 1968 b, Relationship between slope probability density function and the physical optics integral in rough surface scattering. *Proceedings of the IEEE*, **56**, 1728–1729.

BECKMANN, P., and SPIZZICHINO, A., 1963, *The Scattering of Electromagnetic Waves from Rough Surfaces* (New York: Macmillan).

BJERKAAS, A. W., and RIEDEL, F. W., 1979, Proposed model for the elevation spectrum of a wind-roughened sea surface. Technical Memorandum, JHU-APL TG 1328.

BROWN, G. S., 1978, Backscattering from a Gaussian-distributed perfectly conducting rough surface. *IEEE Transactions on Antennas and Propagation*, **26**, 472–482; **28**, 943–946.

BROWN, G. S., 1980, Shadowing by non-Gaussian random surfaces. *IEEE Transactions on Antennas and Propagation*, **28**, 788–790.

BROWN, G. S., 1981, A study of terrain scattering physics. Applied Science Associates, Final Technical Report for Rome Air Development Center, RADC-TR-80-369, Apex NC, February.

BROWN, G. S., 1984, The validity of shadowing corrections in rough surface scattering. *Radio Science*, **19**, 1461–1468.

BURROWS, M. L., 1973, On the composite model for rough-surface scattering. *IEEE Transactions on Antennas and Propagation*, **21**, 241–243.

CARDONE, V. J., 1969, Specification of the wind field distribution in the marine boundary layer for wave forecasting. Report TR 69-1, Geophysical Science Laboratory, New York University, New York.

FUNG, A. K., and EOM, H. J., 1981, Multiple scattering and depolarization by a randomly rough Kirchhoff surface. *IEEE Transactions on Antennas and Propagation*, **29**, 463–471.

GRODY, N. C., 1976, Remote sensing of atmospheric water content from satellite using microwave radiometry. *IEEE Transactions on Antennas and Propagation*, **24**, 155–162.

GUISSARD, A., 1983, Distance measurements correction by radiometry. *Proceedings of the International Geoscience and Remote Sensing Symposium (IGARSS' 83) held in San Francisco, U.S.A. from 31 August–2 September* (New York: IEEE).

GUISSARD, A., 1985, A translation property in rough surface scattering. *Proceedings of the 3rd International Colloquium on Spectral Signatures of Objects in Remote Sensing, held in Les Arcs, France from 16 to 20 December 1985*, ESA SP-247 (Paris: European Space Agency), pp. 123–125.

GUISSARD, A., *et al.*, 1986, Sea surface description requirements for electromagnetic scattering calculations. *Journal of Geophysical Research*, **91**, 2477–2492.

GUISSARD, A., SOBIESKI, P., and GUILLAUME, A. M., 1986, A two-step algorithm for the separate retrieval of ocean surface and atmospheric parameters from microwave radiometers. *Proceedings of the International Geoscience and Remote Sensing Symposium (IGARSS'86) held in Zürich, Switzerland from 8–11 September 1986*, ESA-SP 254, Vol. 2, (Paris: European Space Agency), pp. 1077–1082.

HOLLINGER, J. P., 1971, Passive microwave measurements of sea surface roughness. *IEEE Transactions on Geoscience and Electronics*, **9**, 165–169.

RICE, S. O., 1951, Reflection of electromagnetic waves from slightly rough surfaces. *Communications in Pure and Applied Mathematics*, **4**, 351–378.

SCHANDA, E., 1986, *Physical Fundamentals of Remote Sensing* (Berlin: Springer-Verlag).

SHEARMAN, E. D. R., 1983, Radio science and oceanography. *Radio Science*, **18**, 299–320.

SMITH, B. G., 1967, Lunar surface roughness: shadowing and thermal emission. *Journal of Geophysical Research*, **72**, 4059–4067.

SOBIESKI, P., GUISSARD, A., BAUFAYS, C., VANHOENACKER, D., GUILLAUME, A. M., and VANDER VORST, A., 1986, Study on propagation and inverse scattering. Final Report for European Space Agency, Contract 5285/82, Laboratoire de Télécommunications et d'Hyperfréquences, Université de Louvain, Louvain-la-Neuve, Belgium, March.

THRANE, L., 1978, Evaluation of multi-frequency-microwave-radiometer-system performance for oceanography. *Boundary-Layer Meteorology*, **13**, 373–392.

ULABY, F. T., MOORE, R. K., and FUNG, A. K., 1982, *Microwave Remote Sensing*, Vol. 2 (Reading, Massachusetts: Addison-Wesley).

VALENZUELA, G. R., 1970, The effective reflection coefficients in forward scatter from a dielectric slightly rough surface. *Proceedings of the IEEE*, **58**, 1279.

VALENZUELA, G. R., 1978, *Boundary-Layer Meterology*, **13**, 61–65.

WENTZ, F. J., 1975, A two-scale scattering model for foam-free sea microwave brightness temperatures. *Journal of Geophysical Research*, **80**, 3441–3446.

WENTZ, F. J., 1983, A model function for ocean microwave brightness temperature. *Journal of Geophysical Research*, **88**, 1892–1980.

WRIGHT, J. W., PLANT, W. J., KELLER, W. C., and JONES, W. L., 1980, Ocean wave-radar modulation transfer functions from the West Coast experiment. *Journal of Geophysical Research*, **85**, 4957–4966.

WU, S. T., and FUNG, A. K., 1972, A noncoherent model for microwave emissions and backscattering from the sea surface. *Journal of Geophysical Research*, **77**, 5917–5929.